ACS OMEGA

http://pubs.acs.org/journal/acsodf
Article

Rapid Gluten Allergen Detection Using an Integrated Photoimaging Assay and Ionic Liquid Extraction Sensor

Wen-Hao Chen,[+] Chuan-Chih Hsu,[+] Hsin-Jung Ho,[+] Jill Smith, Seaton Smith, Hui-Yin Huang, Huan-Chi Chang, and Yu-Cheng Hsiao*

Cite This: *ACS Omega* 2024, 9, 49767−49777
Read Online
ACCESS | Metrics & More | Article Recommendations | Supporting Information

ABSTRACT: In recent years, food allergies and food sensitivities have remained critical public health problems that affect approximately 15% of the global population. Wheat is a major food source worldwide, but it is also a common food allergen. Celiac disease is chronic immune-mediated enteropathy triggered by exposure to dietary gluten in genetically predisposed individuals; it can be treated only through strict gluten avoidance. Therefore, rapid gluten detection is crucial for protecting the health of patients. Gluten contains two primary water-insoluble proteins: gliadin and glutenin. Gliadin is a key contributor to celiac disease and poses challenges for sample pretreatment owing to its insolubility, thereby reducing the accuracy and sensitivity of detection systems. Rapid sample processing is a critical problem in gliadin detection. In this report, we developed a gliadin sensor system called the integrated food allergy and microorganism sensor (iFAMs). The iFAMs comprises a gliadin lateral flow chip, a one-pot extraction solution, and an image assay app. The iFAMs enables gliadin extraction and detection in under 2 min with high sensitivity (0.04 mg/kg for gliadin, lower than the regulatory limit of 20 mg/kg). Users can easily measure gluten concentrations in samples and quantify gliadin levels using the smartphone-based image assay app. In samples collected from restaurants, the iFAMs successfully detected hidden gluten within "gluten-free" food items. The compact size and user-friendly design of the iFAMs render it suitable for not only consumers but also clinicians, food industries, and regulators to enhance food safety.

INTRODUCTION

Estimates from the Centers for Disease Control and Prevention (CDC) reveal that more than 50 million people in America experience allergies annually. According to the CDC's National Health Interview Survey, 6.2% of adults and 5.8% of children have food allergies, and approximately US$25 billion is spent on food allergen treatment each year in the United States. Common food allergens include peanuts, nuts, and seafood.[1−3] Even trace amounts of these allergens can trigger acute anaphylaxis, a potentially life-threatening hypersensitivity reaction that requires epinephrine injections. The Food Allergen Labeling and Consumer Protection Act (FALCPA) mandates food labeling to inform consumers about allergenic substances in products. However, mislabeling and cross-contamination in manufacturing continue to pose regulatory challenges. Furthermore, the FALCPA covers only packaged foods and not those served in restaurants. The ability to rapidly test foods for common allergens also remains a major unmet need.

Wheat is a major global food source, but it contains gluten, a food allergen that induces immune responses in individuals with celiac disease and nonceliac gluten sensitivity (NCGS).[4,5] Moreover, wheat gluten includes gliadin; the primary toxic component of gliadin is a 33-mer peptide from alpha-2-gliadin, which contains proline and glutamine amino acid residues. This peptide is often described as the most critical celiac disease immunogenic sequence in gliadin.[6] Currently, the most common treatment for celiac disease involves a strict, lifelong gluten-free diet and/or the consumption of foods with a "gluten-free" label. According to the Codex Standard 118-1979 (adopted by the US Food and Drug Administration, FR Doc. 2013-18813) and European Commission Regulation (EC 41/2009), gluten levels in designated gluten-free foodstuff should not exceed 20 ppm. Currently, gluten-free diets are increasingly popular worldwide regardless of whether individuals have celiac disease.

In people with celiac disease, gluten exposure damages the intestinal villi, impairing the body's ability to absorb essential nutrients for health and growth.[7] Celiac disease is an autoimmune illness caused by an immune reaction to gluten consumption. This chronic immune-mediated enteropathy

Received: September 13, 2024
Revised: November 14, 2024
Accepted: November 20, 2024
Published: December 3, 2024

https://doi.org/10.1021/acsomega.4c08411
ACS Omega 2024, 9, 49767−49777

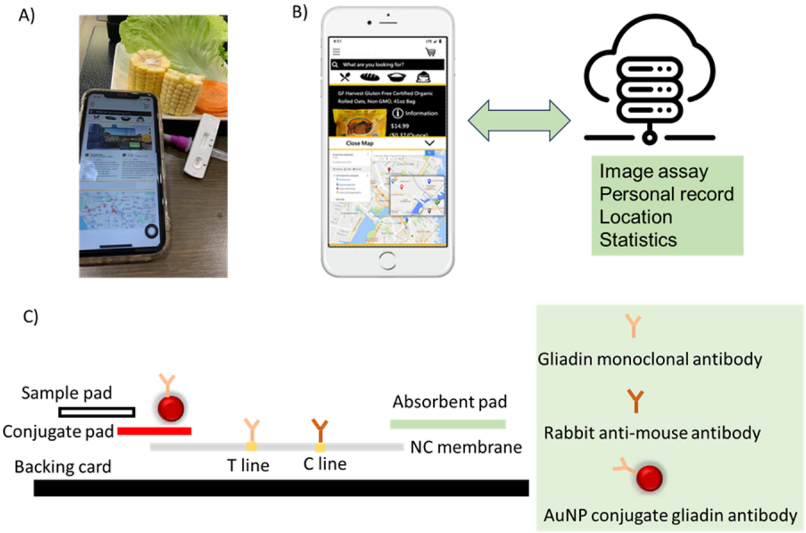

Figure 1. (A) The gluten detection system includes a USB-size detector, a lateral flow-based rapid test chip, and a disposable kit for gluten allergen extraction. (B) Data can be updated to a cloud-based platform for gluten content analysis, and users can capture and upload images of the test strip through their smartphones. (C) Major components of the structure and function of the lateral flow test strip.

occurs in genetically predisposed individuals[8] upon exposure to dietary gluten. In individuals with celiac disease, gluten ingestion activates both innate and adaptive immune responses. These structural changes lead to functional impairment of the intestinal mucosa, which results in symptoms caused by nutrient malabsorption. Gluten comprises several proteins, including alpha-, gamma-, and omega-gliadin as well as high- and low-molecular-weight glutenins. Gliadin is a family of water-insoluble proteins and is the primary contributor to celiac disease.[9−11]

Researchers have used various analytical techniques and devices to analyze gluten levels in processed and unprocessed foods; these techniques and devices include polymerase chain reaction,[12] liquid chromatography−tandem mass spectrometry,[13] microarrays,[14] immunosensors,[15] aptasensors,[16] matrix-assisted laser desorption/ionization time-of-flight mass spectrometry,[17] near-infrared spectroscopy,[18] and electrochemical sensing.[16,19,20] In recent years, enzyme-linked immunosorbent assay (ELISA) and lateral flow assay techniques have been commonly used to comprehensively analyze gliadin content.[21−24] However, efficient gliadin extraction remains a considerable challenge in the aforementioned analytical techniques. Conventional pretreatment processes for extracting gliadin from heat-processed or diluted samples (1:50) after alcohol extraction are time-consuming. Furthermore, diluting samples after alcohol extraction often requires skilled personnel. Regardless of the pretreatment process, conventional gliadin detection methods necessitate specialized equipment to measure gliadin concentrations, making them less user-friendly for consumers.

To address these limitations, we developed a new gliadin detection system called the integrated food allergy and microorganism sensor (iFAMs). The iFAMs effectively extracts gliadin from unprocessed and heat-processed foods and then measures the gliadin concentration through a lateral flow test within 2 min without additional equipment. This sensor is suitable for use by untrained individuals of all ages, even in remote areas lacking advanced medical laboratories. Moreover, users can quantify gliadin concentrations through a smartphone-based image assay app.

The proposed iFAMs comprises a one-pot extraction solution, lateral flow technology, a specialized antibody, and an image assay app. In this study, we generated a monoclonal antibody (against gliadin) from mouse cells, conjugated it with gold nanoparticles (AuNPs), and incorporated it into the lateral flow test strip. A positive test result, signified by the appearance of both test and control lines on the test strip (Figure 1C), was considered to indicate the presence of ≥0.1 ppm of gluten in the sample. A negative test result, signified by the appearance of only the control line, was considered to indicate a gluten concentration of <0.01 ppm (Figure 3A). Furthermore, an analysis conducted using the image assay app revealed that the detection limit for gliadin was 0.04 ppm, demonstrating the high sensitivity of the app.

We optimized the extraction efficiency by employing buffer with an ionic liquid (IL) to achieve rapid one-pot gliadin extraction. Accordingly, the proposed iFAMs can enable users to easily measure gluten concentrations through either the gluten detection sensor or an image assay app. The app also can record and store test results for future reference, which can enable users to track their gluten measurements.

RESULTS AND DISCUSSION

iFAMs Assay. Figure 1A depicts the portable iFAMs system, which contains a gluten sensor chip, an extraction kit, and a smartphone app (Figure 1A,B). The compact design of the proposed iFAMs allows for convenient use in various settings. The detection process involves three simple steps, and the results are displayed in the chip window within 2 min.

First, the allergen is extracted using a specially designed disposable kit containing an IL solution to dissolve gliadin. Because gliadin is a family of water-insoluble proteins derived from wheat, in this study, we optimized the extraction process by employing Tris buffer with 1% imidazolium-based IL [C5DMIM][OMs] (Figure 4).

Second, the gliadin concentration is detected. If gliadin is present in the sample, it binds to the AuNP-conjugated gliadin antibody (AuNP-Ab). This complex is then captured by a gliadin monoclonal antibody immobilized on the test line. Excess AuNP-Ab is captured by a rabbit antimouse antibody

https://doi.org/10.1021/acsomega.4c08411
ACS Omega 2024, 9, 49767−49777

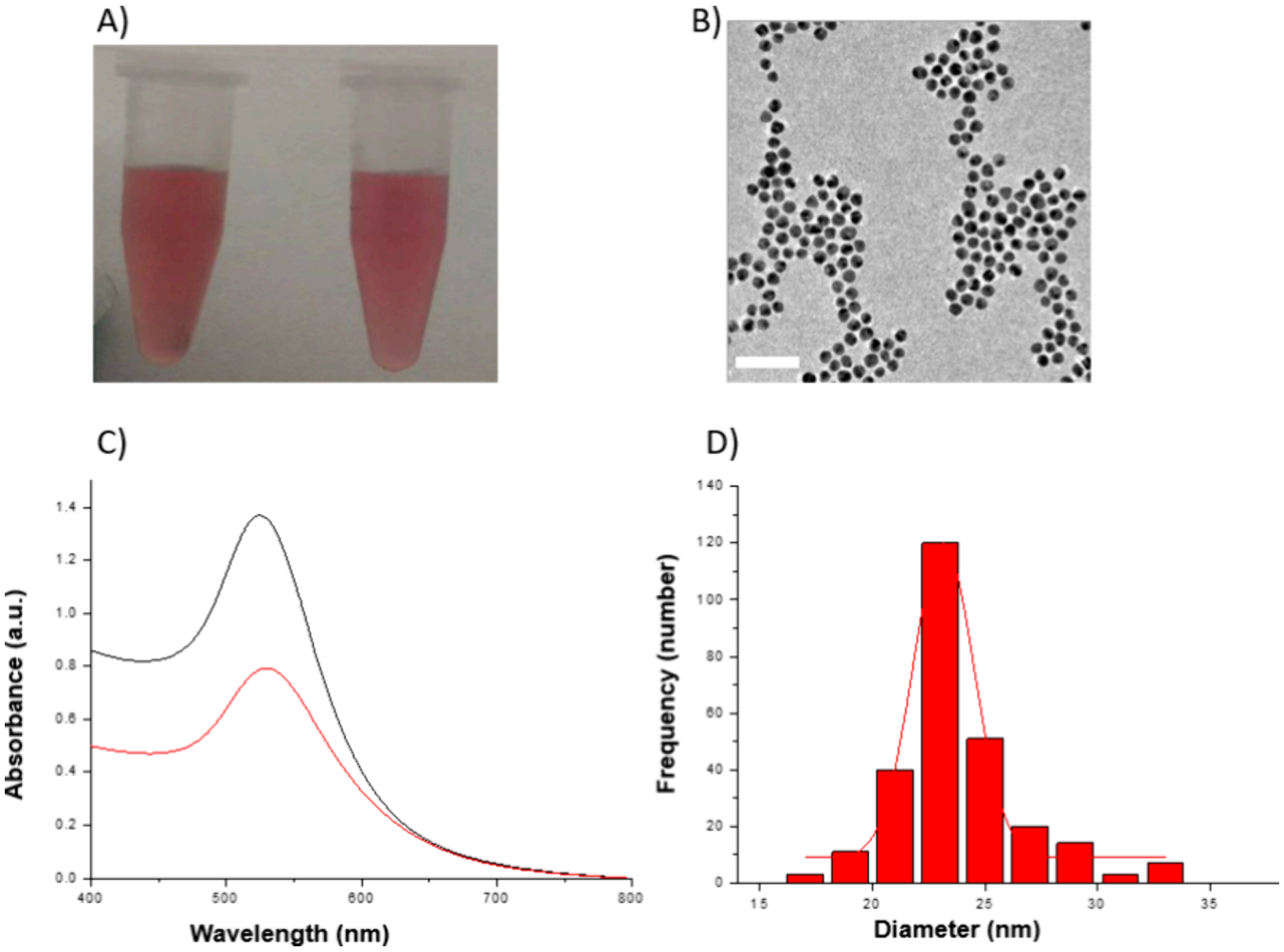

Figure 2. (A) AuNPs with (right)/without (left) antibody coating. (B) TEM image of Au particles (scale bar, 100 nm). (C) UV−VIS spectra of AuNPs with (red line)/without (black line) antibody coating. (D) Size distribution of AuNPs based on diameter measurements.

on the control line. The appearance of two red lines on the gluten sensor chip indicates a positive result, and the appearance of only the control line signifies a negative result (Figure 1C).

Finally, the smartphone app is used to measure the gliadin concentration. The app captures an image of the test strip and uploads it to the cloud, where a standard curve of gliadin concentration is used to normalize and calculate the gliadin concentration on the basis of the color intensity of the test and control lines. The app also records the time and location of the test (Figure S2).

Characterization of Antibody Conjugated with AuNPs. AuNPs exhibit a unique local surface plasmon resonance effect that is sensitive to particle size and surface chemistry.[25,26] Accordingly, the proposed iFAMs leverages this effect through the use of citrate-reduced AuNPs. We synthesized AuNPs through several steps: nucleation (reduction of $HAuCl_4$ to Au atoms),[27] followed by the growth and agglomeration of these atoms into nanoclusters, resulting in a red AuNP solution (Figure 2A, left panel). The AuNPs were then conjugated with the gliadin antibody (Figure 2A, right panel). Conjugation with the antibody did not engender a considerable color shift in the AuNPs. Furthermore, the size distribution and average diameter of the AuNPs were characterized using ultraviolet−visible (UV−VIS) light spectrophotometry and atomic force microscopy (AFM; Figure 2B,C). The UV−VIS spectra revealed narrow absorption peaks for unconjugated AuNPs (521 nm) and antibody-conjugated AuNPs (523 nm). The spherical morphology of the AuNPs was confirmed by the AFM results (Figure 2B). ImageJ software was used to analyze the AFM images, and the results indicated a uniform size distribution with an average diameter of approximately 24 nm (Figure 2D). Dynamic light scattering was also used to measure the size of the AuNPs. The hydrodynamic diameters of the unconjugated and antibody-conjugated AuNPs were 25 and 40 nm, respectively.

Optimal Antibody Concentrations for Conjugation with AuNPs. The pH value influences the conjugation of antibodies to the AuNPs. We investigated the effect of pH on antibody−AuNP conjugation.[28] Successful conjugation was defined as the absence of notable color shifts upon antibody or salt addition. Our experiments revealed that the optimal pH for conjugation was 8. At this pH, the highest stable concentration of the antibody-conjugated AuNPs in solution was achieved when the antibody concentration was 1 μg/mL. We determined this by observing color changes in AuNP solutions containing different antibody concentrations in the presence of NaCl. Moreover, we validated these results by measuring and comparing the UV−VIS absorption spectra of the synthesized AuNPs. Owing to the sensitivity and unique properties of

https://doi.org/10.1021/acsomega.4c08411
ACS Omega 2024, 9, 49767−49777

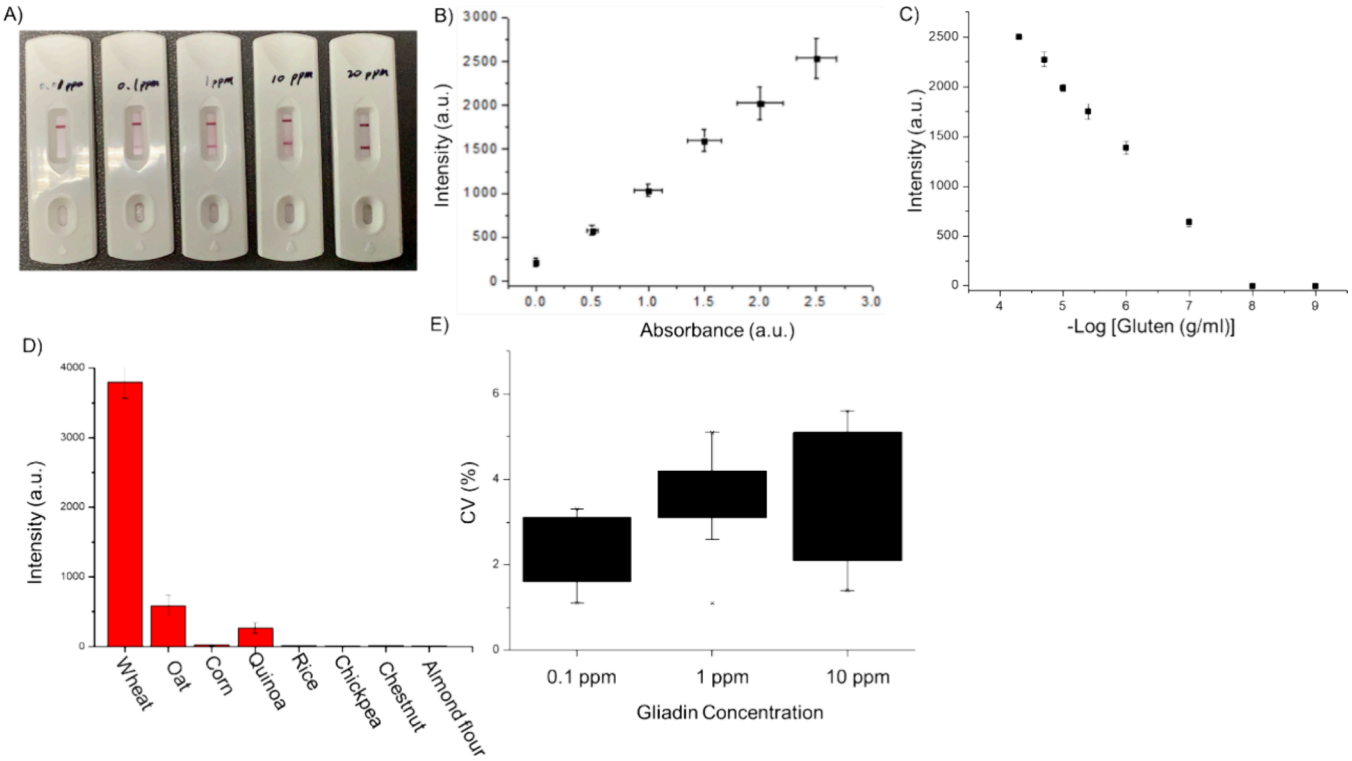

Figure 3. (A) iFAMs gluten test (left to right: 0.01, 0.1, 1, 10, and 20 ppm) results. (B) The iFAMs results exhibited an excellent match with the ELISA results (R^2 = 0.995). (C) Samples with varying doses of gliadin were analyzed using the iFAMs, and response curves were generated. The detection limit was below the relevant elicit dose. (D) Specificity of the iFAMs for different flour samples. (E) The iFAMs was noted to be highly reproducible. Both the intra-assay and interassay variations were <6%.

AuNPs, changes in absorbance spectra can indicate surface binding events.[29] In our study, when the antibody concentration was 1 μg/mL, the absorption peak at 520 nm increased and exhibited a shift toward longer wavelengths. This spectral change confirms the interaction between the antibodies and the AuNP surface (Figure 1C).

Analytical Performance. To quantify the gliadin concentration within the iFAMs rapid test, we developed an image assay system for analyzing test results. This system facilitates the evaluation of the analytical performance of the proposed iFAMs for rapid gluten detection. First, response curves were generated by varying the gliadin concentrations. These curves were then incorporated into the iFAMs image assay system as lookup tables, enabling quantitative analysis. The iFAMs assay demonstrated high sensitivity, precision, and quantitative accuracy. The limit of detection for gliadin was 0.04 ppm, which is lower than the eliciting dose thresholds for gluten allergens (20 ppm). Intra-assay variations were assessed by measuring eight replicates of three different standard concentrations (0.1, 1, and 10 ppm). The results revealed excellent intra-assay precision, with variations below 6% (Figure 3D). Furthermore, interassay variations were evaluated and found to be less than 7%. For comparative purposes, the same samples were analyzed by using the conventional ELISA technique. The iFAMs results exhibited a strong correlation with the ELISA results (Figure 3A, R^2 = 0.995). Notably, the iFAMs assay offered a considerable advantage in terms of speed, delivering results within 2 min, when compared with the ELISA technique, which required a 3 h analysis time.

Sensitivity of iFAMs. To assess the sensitivity of the iFAMs, we tested eight gluten concentrations (0.001, 0.01, 0.1, 1, 5, 10, 15, and 20 ppm) in triplicate. A visible pink color appeared along the test line as the gluten concentration was increased from 0.01 to 20 ppm (Figure 2B). Furthermore, the color intensity of the test line increased with the gluten concentration (Figure 3B).

We used the following equation to calculate the detection limit of the iFAMs: $S_{dl} = S_{reag} + 3\sigma_{reag}$, where S_{dl} is the detection limit, S_{reag} is the signal of the reagent blank, and σ_{reag} is the standard deviation of the reagent blank. The calculation indicated that the detection limit was 0.04 ppm. Moreover, the entire test procedure was completed within 2 min.

Specificity of iFAMs. Specificity is a crucial metric for biosensors. To evaluate the specificity of the proposed iFAMs, we tested flour samples derived from various cereals: wheat, oat, corn, quinoa, rice, chickpea, chestnut, and almond. We observed a red line on the test strip only for the gluten-containing cereals: wheat, oat, and quinoa. Moreover, the red line for wheat flour appeared within 2 min, likely due to its high gluten concentration (Figure 3C). Each sample was tested six times under the same experimental conditions.

Despite being intrinsically gluten-free, both oat and quinoa showed traces of gluten in our analysis. This finding is likely a result of cross-contamination, a common problem with "high-risk" gluten-free grains. Cross-contact often occurs during growing, harvesting, or processing alongside gluten-containing grains such as wheat, barley, and rye.[30−32]

Gliadin Solubility in Different Buffer Systems. To investigate gliadin solubility, we added 3 g of gluten (excess amount, sourced from Sigma-Aldrich) to 10 mL of various buffer solutions [Tris, phosphate-buffered saline (PBS), citric acid, carbonate, and water]. The mixtures were homogenized by stirring for 30 min and then allowed to rest for 5 min. After the extraction process, all samples were centrifuged at 8,500

https://doi.org/10.1021/acsomega.4c08411
ACS Omega 2024, 9, 49767−49777

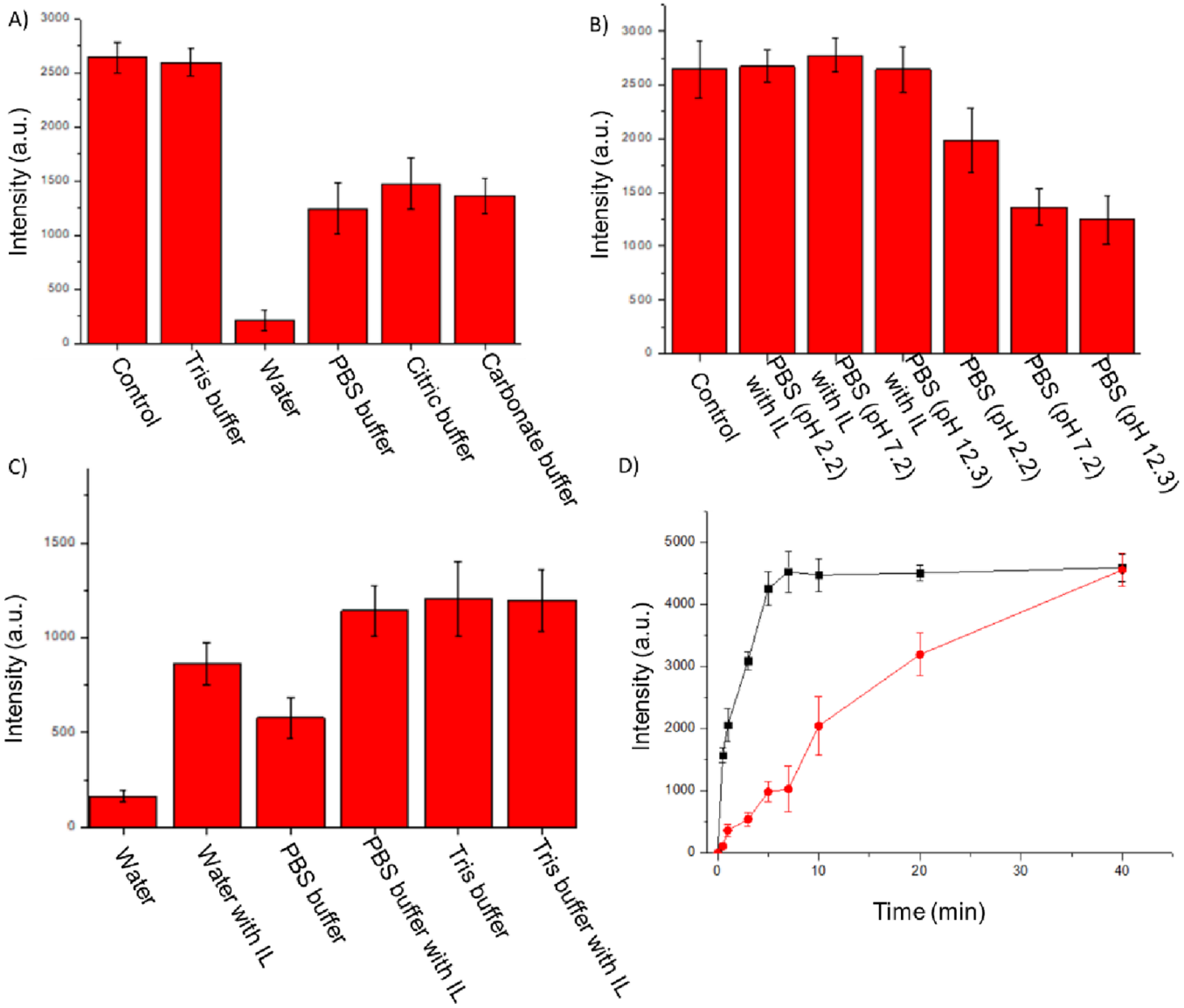

Figure 4. (A) Different types of extraction buffers were used for gliadin extraction. A control solution was prepared using a 75% alcohol solution, which was subsequently diluted 50 times in PBS buffer. (B) Gliadin extraction test conducted using PBS buffer solutions of varying pH levels and with/without IL ([PDMIM][MOS]). (C) Effect of antibody binding with gliadin in different buffer solutions. (D) Time dependency of extraction of gliadin from Tris buffer with/without IL (the black line denotes Tris buffer with 1% IL; the red line denotes Tris buffer).

rpm for 3 min to remove any particulates. The supernatant solutions were then passed through a 0.22-μm filter to obtain clarified solutions for further analysis. Ethanol solution (75 wt %) was used as the control. To ensure an accurate comparison with the other samples, the control solution was diluted five times with deionized water prior to analysis. The iFAMs was used to quantify the gliadin concentration in all clarified samples (Figure 4A).

Alcohol-based solutions are commonly used for gliadin extraction,[33] and Tris buffer is known for its ability to enhance gliadin solubility.[34] Our results (Figure 4A) demonstrated that the gliadin solubility levels were the highest in alcohol and Tris buffer and poor in water alone. Moreover, we observed that PBS, citric acid buffer, and carbonate buffer could dissolve gliadin. These findings support the observation that salts increase gliadin solubility in water.[35]

Gliadin Solubility in pH Buffer with and without IL. To investigate the effect of pH and IL on gliadin solubility, we added 3 g of gluten (excess amount, sourced from Sigma-Aldrich) to 10 mL of pH-adjusted buffer solutions (pH 2.2, 7.2, and 12.3) with and without IL. The mixtures were homogenized by stirring for 30 min and then allowed to stand for 5 min. After centrifugation at 8500 rpm for 3 min and filtration through a 0.22 μm filter, we used the proposed iFAMs to quantify the gliadin concentration (Figure 4B). A 75% alcohol solution (diluted five times with deionized water) served as the control.

As expected, acidic pH enhanced gliadin solubility, particularly in PBS buffer.[36] However, the addition of IL considerably increased the gliadin solubility across all tested pH values in PBS, demonstrating the positive effect of IL on extraction efficiency.

Environmental Effect. Ionic strength and pH can influence antibody binding affinity in some cases.[37,38] Accordingly, we investigated the potential effects of ionic strength and pH on antibody binding affinity. To isolate the

https://doi.org/10.1021/acsomega.4c08411
ACS Omega 2024, 9, 49767−49777

effects of different buffer solutions, we first prepared a gluten standard solution using 75% alcohol. We then diluted this standard solution (1 mL) with various buffer solutions (4 mL) containing water, PBS, or Tris (with or without IL) to minimize the influence of alcohol on antibody binding. The resulting solutions were analyzed using the iFAMs (Figure 4C).

The results demonstrated a considerable difference in signal intensity between water with and without IL. Water alone exhibited a low signal intensity level, likely owing to gliadin precipitation. However, the addition of IL considerably enhanced the signal intensity level, suggesting that IL enhances gliadin solubility in water. A similar, although less pronounced, effect was observed in PBS with and without IL. The presence of IL did not considerably alter the signal intensity in the Tris buffer solution.

Time Dependency of Gliadin Solubility in Tris Buffer with and without IL. IL shows promise as a solvent for organic transformations. We investigated the effect of IL on gliadin solubility in Tris buffer over time.

As illustrated in Figure 4D, gliadin solubility in Tris buffer alone gradually increased with time, with the solubility level peaking after 40 min at room temperature (red cycle). Moreover, the addition of 1% IL considerably enhanced gliadin solubility with maximum solubility occurring within just 5 min (black square). Our results demonstrate that the addition of the IL $[C5DMIM][MSO]_{aq}$ considerably improved gliadin extraction efficiency in Tris buffer. The extraction effectiveness observed with IL was more than eight times greater than that with Tris buffer alone. This finding demonstrates the ability of the IL to enhance gliadin solubility. For gluten detection, effective extraction directly influences the sensitivity of the assays. Therefore, the use of Tris buffer with an IL affords a rapid and highly efficient method for gliadin extraction, potentially improving the sensitivity of gluten tests.

Gliadin Recovery Rate with iFAMs. Recovery rate is a crucial metric for evaluating extraction systems; this is because it reflects the effectiveness of extracting a target substance from a sample. In this study, we assessed the gliadin recovery performance of the iFAMs.

Rice noodles constitute a well-known gluten-free food, and they were selected as the sample for the recovery test. Initially, rice noodles were assessed for the gliadin absence through ELISA. Subsequently, a 10 ppm gliadin solution was added to the rice noodles, and the solution was removed via vacuum to prepare the gliadin sample standard.

The iFAMs was used to extract gliadin from the standard sample, and the gliadin concentration was measured using ELISA. The resulting data are listed in Table 1. A 100% recovery rate was defined as a recovery of 200 ppm of gliadin. Across five repetitions of the recovery test using the iFAMs, the average recovery rate achieved by the iFAMs for a 1 wt % ionic solution was determined to be 97.8%.

Table 1. Recovery Test of the iFAMs

	standard gluten (ppm)	extraction gliadin (ppm)	recovery (%)
1	10	9.3	93%
2	10	9.6	96%
3	10	10.5	105%
4	10	9.4	94%
5	10	10.1	101%
average	10	9.78	97.8%

Testing of Commercially Available Products. The lateral flow test for gliadin is a rapid and user-friendly assay method. The R-Biopharm gliadin test is the only strip-based assay for gliadin detection using the G5 antibody. The sensitivity and specificity of the G5 antibody contribute to the high sensitivity of the R-Biopharm gliadin test. However, the pretreatment process in the R-Biopharm gliadin test still requires sample heating and is time-consuming. Nevertheless, the R-Biopharm gliadin test remains widely used for gliadin detection.

In this study, we compared the performance of the iFAMs with that of the R-Biopharm gliadin test in processing food samples, and the results are listed in Table 2. The results revealed a high level of consistency between the iFAMs and the R-Biopharm gliadin test. This demonstrates that the iFAMs is effective in detecting gliadin during food processing.

Table 2. Lateral Flow Test of Processing Food Using the iFAMs and R-Biopharm Gliadin Test

	label GF	iFAMs	R-Biopharm (R7003)
Guerrero Tostatas	yes	0 ppm	<5 ppm
Krusteaz GF All-Purpose Flour	yes	0 ppm	<5 ppm
Krusteaz GF Honey Cornbread Mix	yes	0.4 ppm	<5 ppm
Sprouts GF Steel Cut Oats	yes	0 ppm	<5 ppm
Pillsbury GF Choc Fudge Brownie Mix	yes	0 ppm	<5 ppm
Lay's Stax Mesquite Barbecue Chips Chips McCornmic	yes	0 ppm	<5 ppm
Kelloggs Multi-grain Club Crackers	no	>40 ppm	>40 ppm
Smarties Candy Bracelate	no	0 ppm	<5 ppm
Fritos Chili Cheese Chips	no	0 ppm	<5 ppm
mild taco seasoning	no	0 ppm	<5 ppm
Cap't Crunch Berries	no	0.6 ppm	<5 ppm

We further evaluated the performance of the iFAMs by testing various consumer food products including packaged staples and desserts. Small samples (40 mg) were collected, and solid foods were crumbled before analysis. We compared the performance of the iFAMs with that of ELISA and the Ecove gluten sensor, another rapid test with a one-pot extraction technology. Ecove claims higher sensitivity (1 ppm) than ELISA. However, our test results (Table 3) revealed consistency between the iFAMs and ELISA. In some cases, where the gliadin concentration was below the sensitivity threshold of ELISA (2 ppm), detection may not occur. Overall, iFAMs and ELISA exhibited a high level of consistency. However, the performance of the Ecove gluten sensor was not satisfactory, particularly evident in its inability to detect gliadin in toast and noodle samples. Even after three repeated tests on the noodles and toast, Ecove failed to provide a clear positive result.

Furthermore, we tested samples with fermentation (beer and sauce) and detected gliadin in these samples (Table 4). We attempted to use the iFAMs for the detection of gliadin-derived peptides (33 amino acids); however, the iFAMs was ineffective in detecting these peptides (data not shown).

Additionally, using the iFAMs interface with a smartphone app, we tracked personal dietary intake and recorded gluten data with timestamps in a cloud server. The server documented the results alongside local restaurant information. These data

https://doi.org/10.1021/acsomega.4c08411
ACS Omega 2024, 9, 49767−49777

Table 3. Food-Processing Test Using the iFAMs, ELISA, and Ecove Gluten Sensor

	iFAMs	ELISA	Ecove[a]
Ferrero	7 ppm	8 ppm	N.D.
bagel	>40 ppm	>40 ppm	yes
fried dumplings	>40 ppm	>40 ppm	N.D.
toast	>40 ppm	>40 ppm	N.D.
Lay's Stax Original Potato Chips	0.5 ppm	0 ppm	N.D.
Nestle Nesquik Chocolate Syrup	0.6 ppm	0 ppm	N.D.
M&M's Crispy Milk Chocolate Bar	1.8 ppm	2.2 ppm	N.D.
Campbell's Chunky New England Clam Chowder	7.6 ppm	6.4 ppm	yes
Lindt Swiss Classic Milk Chocolate	3.2 ppm	2.1 ppm	N.D.
S&B Golden Curry Sauce with Vegetables Mild	10.2 ppm	9.8 ppm	yes
Hershey's Cookies 'N' Cream Candy Bar	7.6 ppm	9.4 ppm	yes
Nestle Kit Kay Chunky Peanut Butter Chocolate	>40 ppm	>40 ppm	yes
Barilla Capellini no. 1	>40 ppm	>40 ppm	N.D.
Lotus Biscoff Spread Crunchy	>40 ppm	>40 ppm	yes
Munchy's Oat Krunch Crackers Strawberry & Blackcurrant	>40 ppm	>40 ppm	yes
Bento Squid Seafood Snack Original Thai Chili Sauce	>40 ppm	>40 ppm	yes
Big Lost: Crazy Woman	0 ppm	0 ppm	N.D.
Big List: Wild Man	0 ppm	0 ppm	N.D.
Pine Ridge: Barbecue & Dipping Sauce	0 ppm	0 ppm	N.D.
Pine Ridge: Jalapeno Barbecue & Dipping Sauce	0 ppm	0 ppm	N.D.
Pine Ridge: Sweet Mustard Sauce	0 ppm	0 ppm	N.D.
Jackson Hole Still Works: Great Gray Gin	0 ppm	0 ppm	N.D.
Jackson Hole Still Works: Vodka	0 ppm	0 ppm	N.D.
Jackson Hole Still Works: Absaroka Double Cask Gin 49	0 ppm	0 ppm	N.D.
Budweiser beer	12.6 ppm	11.4 ppm	yes
Lee Kum Kee Premium Oyster Flavored Sauce	3.1 ppm	2.4 ppm	N.D.
Toblerone Swiss Milk Chocolate with Honey and Almond Nougat	0.4 ppm	0 ppm	N.D.

[a]N.D., not determined.

Table 4. Comparison of the iFAMs with Other Lateral Flow Assays

type of assay	LOD (ppm)	reference
iFAMs	0.04	
3M Gluten Protein Rapid Kit	5	39
GlutenTox Sticks	3	40
EZ Gluten	10	41

were then used to generate an evidence-based restaurant map, which can be shared online.

CONCLUSIONS

Food allergies represent a crucial public health concern in the United States. Approximately 30% of allergic children experience multiple allergies, with nearly 203,000 allergy-related emergency department visits annually, including 90,000 cases of anaphylaxis. Gluten-related sensitivities, including celiac disease, NCGS, and gluten intolerance, affect a considerable portion of the population (approximately 5%).[4−6] Although a gluten-free diet is essential for managing these conditions, implementation remains challenging, owing to frequent cross-contamination. Proper diagnosis, food allergen identification, and real-time monitoring are crucial for reducing the negative effects of food allergies.

To address these challenges, we developed a point-of-care food testing system, namely, the iFAMs, for precise gluten detection; this sensor can help individuals make informed decisions or choices and can eliminate unnecessary dietary restrictions. Moreover, the proposed iFAMs is compact, rapid, user-friendly, and quantitative. It is also cost-effective, with assay costs under $5 per antigen (Figure S1) and no additional equipment requirements. The iFAMs is highly adaptable and outperforms other consumer gluten detection methods because it eliminates complicated pretreatment steps and multisolvent requirements. Its size and ease of use enable widespread application in various settings, including safeguarding consumer health, quality control, environmental monitoring, and supply chain oversight.

Compared with other rapid tests and ELISA techniques, the proposed iFAMs offers advantages such as ease of use, speed, accessibility, and broad applicability (Figure S3). These features make it a promising tool for various food safety applications. We envision expanding the iFAMs platform to detect other common food allergens (e.g., peanuts, nuts, milk, and seafood), creating a comprehensive detection panel. This sensor could be used to ensure food safety, verify food origins, confirm the absence of contaminants, and support dietary restrictions for various needs including religious purposes. Furthermore, through modification of the affinity ligands, the iFAMs assay format could potentially be adapted to detect a wide range of analytes such as small molecules, toxins, and nucleic acids. This versatility opens up possibilities for applications beyond food testing, offering a powerful tool for various analytical needs.

We believe that the portable iFAMs has the potential to revolutionize food analysis by offering more rigorous and evidence-based methods for consumer protection. It can help reduce accidental allergen exposure and identify problems within the food supply chain.

MATERIALS

Reagents and Solvents. All solutions and samples were prepared by using deionized water with a resistivity of 18.2 Ω cm^{-1} from a Millipore Milli-Q water purification system (Millipore). Hydrogen tetrachloroaurate trihydrate ($HAuCl_4 \cdot 3H_2O$), imidazole, propanol, methanesulfonyl chloride, gluten from wheat, and citric acid were procured from Sigma-Aldrich. Tris buffer, PBS buffer, sodium bicarbonate, hydrochloride, sodium hydroxide, potassium chloride, sodium dihydrogen phosphate, sodium hydrogen phosphate, and sodium chloride were purchased from ACOS. Dichloromethane, acetonitrile, methanol, and ethanol were purchased from Tedia. Nitrocellulose membranes (Hi-Flow Plus 120, Merck Millipore), sample pads (cellulose fiber, Merck Millipore), conjugate pads (cellulose fiber, Merck Millipore), absorbent pads, adhesive backing cards, and goat antimouse IgG were obtained from Rojan Azma Co. (Tehran, Iran). Trisodium citrate dihydrate, bovine serum albumin, Tween 20, phosphate buffer solution, PEG20000, glucose, and 0.22 μm filters were purchased from Merck.

https://doi.org/10.1021/acsomega.4c08411
ACS Omega 2024, 9, 49767−49777

METHODS

Preparation of Different Buffer Types. *Preparation of PBS Buffer Standard and PBS with 10% IL.* For the standard, we prepared 800 mL of distilled water in a Duran bottle. Next, 8 g of NaCl, 1.44 g of Na_2HPO_4, 0.2 g of KCl, and 0.24 g of KH_2PO_4 were added to the water. The pH was adjusted to 7.4 or 7.2 (depending on the application) by using HCl and adding deionized water until the total volume reached 1 L, yielding a standard solution.

For PBS with 10% IL, we added 10 g of IL to 990 mL of the PBS standard solution to prepare a PBS−IL solution.

Preparation of Tris Buffer. For the standard, we prepared 800 mL of distilled water in a suitable container, to which we added 121.14 g of Tris base, and then adjusted the solution to the desired pH by using HCl (typically around pH 7.0). Next, we added distilled water until the volume reached 1 L to obtain a standard solution.

For Tris buffer with 10% IL, we added 10 g of IL to 990 mL of Tris buffer to prepare Tris buffer with 10% IL at room temperature.

Carbonate Buffer Preparation. For the standard, we added 1.05 g of sodium bicarbonate and 9.274 g of sodium carbonate (anhydrous) to 800 mL of distilled water in a suitable container. Subsequently, distilled water was added to the solution until a total volume of 1 L was achieved, yielding the standard solution.

For carbonate buffer with 10% IL, we added 10 g of IL to 990 mL of the standard solution in a suitable container.

Citric Buffer Preparation. For the standard, we added 24.269 g of sodium citrate dihydrate and 3.358 g of citric acid to the solution and 800 mL of distilled water in a suitable container. The solution pH was adjusted to the desired level using 0.1 N HCl (typical pH of approximately 6.0) as the standard solution.

For citric buffer with 10% IL, we added distilled water to 990 mL of the standard solution in a suitable container until the total volume reached 1 L.

ELISA. The wheat/gluten (gliadin) ELISA kit (Crystal Chem, AOAC no. 011804) was used in this study. Initially, 1 g of the homogenized mixture was suspended in 10 mL of 40% ethanol. Subsequently, the suspension was mixed for an additional 5 min to ensure thorough homogeneity. The samples were then centrifuged for 10 min at a rate of 2500*g*. The resulting particle-free solution was diluted at 1:50 in 1× diluent buffer. All materials were brought to room temperature (20−25 °C) before use. The standards and samples were assayed in duplicates. Specifically, we added 100 μL of samples or standards to the antibody-coated microplate and incubated the plate at room temperature for 20 min. Each well was aspirated and washed three times with 1× wash buffer (300 μL) by using a squirt bottle or manifold dispenser. The remaining liquid was completely removed after each wash to ensure optimal performance. We added 100 μL of the antibody conjugate to each well and then incubated the plate at room temperature for 20 min on a microplate shaker. Each well was aspirated, and the washing process was repeated. The 3,3′,5,5′-tetramethylbenzidine substrate was brought to room temperature, and 100 μL of the substrate was added to each well (including blank wells). The plate was incubated for 20 min at room temperature in the dark. We added 100 μL of stop solution to each well (including blank wells). Optical density was immediately measured with a microplate reader at 450 nm.

AuNPs were synthesized using citric acid to reduce Au ions in a water solution.[42] Specifically, 100 mL of $HAuCl_4$ (0.02%) was refluxed with constant stirring, after which 3 mL of a 1% trisodium citrate solution was immediately added to the conical flask with continuous stirring. Within 2−5 min, the initial pale yellow-colored solution turned colorless and changed to bluish-gray. After an additional 5 min, the solution turned reddish-purple, indicating the formation of AuNPs. The solution was stirred for another 10 min and then cooled to room temperature.

IL Synthesis. An imidazolium-based IL was synthesized through an S_N2 reaction with 1-methylsulfonic pentane.[43] Pentanol (1 equiv) and triethylamine (1.2 equiv) were added to a reaction bulb, followed by the addition of 30 mL of dichloromethane. The mixture was stirred in an ice bath for 5 min. Methanesulfonyl chloride (MsCl) at 1.1 equiv was slowly added dropwise into the reaction bulb to form a mixture. Subsequently, the ice bath was removed and the mixture was allowed to react at room temperature for 20 min to yield the initial reaction mixture.

The initial reaction mixture was then extracted three times with a 10% (w/v) aqueous solution of citric acid (water phase), followed by three instances of extraction with a 10% aqueous solution of sodium hydrogen carbonate ($NaHCO_3$) to produce an extract. After extraction, the solvent in the extract was removed by concentration under reduced pressure. 1,2-Dimethylimidazole at 0.9 equiv and 50 mL of acetonitrile were added, and the mixture was heated to 60 °C and maintained at this temperature for 12 h to generate a second reaction mixture. Subsequently, the solvent in the second reaction mixture was removed by concentration under reduced pressure to obtain the first crude product. This crude product was then extracted with hexane and dried at concentration under reduced pressure.

The nuclear magnetic resonance spectrum of [C5DMIM]-[OMs] (200 MHz, $CDCl_3$) displayed signals at 0.86−0.88 (3H, t), 1.86−1.91 (4H, m), 2.85 (3H, s), 3.85−3.87 (2H, t), 3.91 (3H, s), 4.12 (3H, s), 7.84−7.85 (1H, d), and 7.87−7.88 (1H, s).

Ethics Statement. Vertebrate animal protocols were implemented in accordance with the Ethics of Animal Experimentation of the National Health Research Institutes, Taiwan, and approved by Taipei Medical University (approval number 112029-A-S01).

Immunization of Mice. Female gestating CD1 outbred mice were obtained from Charles River and maintained on a gluten-free diet from gestational day 15 onward. The offspring continued to receive the same gluten-free diet after weaning. Gluten-free raised animals were used for the immunization experiments at 8 weeks of age. The mice were housed in a specific pathogen-free animal facility at the Taipei Medical University, Taiwan. Systemic immunizations were performed via intraperitoneal injection. Each group consisted of two animals. The animals received three doses of either 100 μg of gliadin or 100 μg of glutenin, each coadministered with 50 μg of muramyl dipeptide (MDP; Sigma-Aldrich) in 200 μL of PBS (pH 7.4; 137 mM NaCl, 2.7 mM KCl, 10 mM Na_2HPO_4, and 2 mM KH_2PO_4). Doses were administered at 3 week intervals. Control animals ($n = 2$) received 200 μL of PBS with 50 μg of MDP. Blood samples were collected from all mice via the tail vein 2 days before immunization. Thirteen days after the final immunization, blood was collected through a terminal cardiac puncture, and the mice were euthanized through CO_2

https://doi.org/10.1021/acsomega.4c08411
ACS Omega 2024, 9, 49767−49777

inhalation. Blood was allowed to clot at 4 °C overnight. Sera were then separated by centrifugation (15,000*g*, 15 min, room temperature), aliquoted, snap-frozen in liquid nitrogen, and stored at −80 °C. [The ELISA assay will be used to determine the antibody binding to gliadin. A specific antibody pair (E1 and E2) was selected for subsequent flow cytometry experiments.]

Preparation of a Lateral Flow System. The test strip was constructed using a sample pad, conjugate pad, nitrocellulose membrane, absorbent pad, and adhesive backing cards. To form the test and control lines, gliadin monoclonal antibody (E1) (60 μg/mL) and goat antimouse IgG (100 μg/mL, Sigma-Aldrich) were dispensed onto the nitrocellulose membrane at a 6 mm distance. Sample pad preparation involved pH optimization and blocking of buffer composition. The pad was treated with PBS containing 5% (w/v) bovine serum albumin, 0.5% Tween 20, 5% poly(ethylene glycol), and 0.05% (w/v) NaN_3, followed by incubation for 30 min. The treated pad was then rinsed with PBS buffer and dried overnight at 37 °C. The conjugate pad was prepared through soaking in the conjugate solution and incubated overnight at 37 °C.

Preparation of a AuNP-Conjugated Antibody. Passive adsorption is a commonly used technique for conjugating antibodies to AuNPs. In this procedure, we added 100 μL of gliadin antibody (E2) solution (1 μg/mL) to an Eppendorf tube containing 1 mL of AuNPs. The mixture was rotated for 30 min to facilitate antibody adsorption. To block any remaining binding sites on the AuNP surface, we added 10% bovine serum albumin. Centrifugation (10,000 rpm for 30 min at 4 °C) was used to separate the antibody-conjugated AuNPs from unbound reagents. This centrifugation step was repeated twice to ensure thorough washing. Finally, the obtained pellet was resuspended in 1% bovine serum albumin and stored at 4 °C until further use.

Specific Test of Sample Preparation. Gluten was extracted from designated food samples (wheat, oat, corn, quinoa, rice, chickpea, chestnut, and almond flour) using 75% (v/v) ethanol. The supernatant was filtered through a 0.22 μm filter and diluted with PBS buffer to create a 100 ppm gliadin standard solution. We prepared a series of gluten concentrations (0, 0.001, 0.1, 1, 5, 10, 20, and 40 ppm) by serially diluting the stock solution with PBS buffer.

Preparation of Gliadin Standard Solution. Gliadin extraction from the flour samples was performed as follows: 1 g of flour was stirred with 10 mL of a 75% (v/v) ethanol solution to achieve a homogeneous mixture. The solution was then centrifuged at 6000 rpm for 10 min at room temperature, and the supernatant was subsequently diluted to 0.01, 0.1, 1, 5, 10, 20, and 40 ppm of gliadin standard solution using PBS buffer (measured by ELISA).

Image Assay System. We developed a functional Web site for analysis color intensity in lateral flow to facilitate system operation and data collection and recording. This app enables users to capture sample images, record relevant measurement data (including timestamps, estimated analyte concentration, and Global Positioning System location), and store the information securely in a cloud-based storage solution (Google Drive).

iFAMs Assay. We placed 20 mg of the sample into the iFAMs extraction channel and closed the cover before shaking it three times. Subsequently, the small cover was opened slightly, and some solution was dropped into the sample window on the iFAMs chip. The test result appeared in the result window after 1.5 min. Subsequently, an image was captured through the iFAMs app, and the image was updated. The gliadin content was then displayed in the app after 15 s.

Preparation of Real Samples. Food samples were collected from local supermarkets and restaurants. For each sample, the following procedure was used: 20 mg of the food sample was combined with 1 mL of extraction buffer and shaken three times to facilitate extraction. A few drops of the extracted sample liquid were added to the iFAMs chip, and the test result was observed in the result window after 2 min.

Statistical Analysis. All calculated data are presented as the means ± standard deviations. A p value of <0.05 was considered significant.

Gliadin Solubility in Different Buffer Systems. We evaluated the effectiveness of different buffer solutions for gluten extraction from the flour samples. We mixed 1 g of flour with 10 mL of each buffer solution (PBS, Tris, carbonate, and citrate) to obtain homogeneous mixtures, which were stirred for 6 h at room temperature. Each mixture was then centrifuged at 6000 rpm for 10 min at room temperature, and the supernatant, containing the extracted gluten, was collected from each sample. Finally, the gliadin concentration in each supernatant was measured by using the iFAMs system.

Gliadin Solubility in pH Buffer with and without IL. We prepared PBS buffer solutions at pH 2.2, 7.2, and 12.3 and adjusted the pH using HCl and NaOH. Additionally, separate buffer solutions were prepared by adding 1 mL of IL to 9 mL of each PBS buffer solution (pH 2.2, 7.2, and 12.3). Then, 1 g of flour was mixed with 10 mL of each buffer solution, and the mixture was stirred for 6 h to obtain a homogeneous mixture. Precipitates were then removed by filtering the mixture through a 0.22 mm filter at room temperature. Finally, the gliadin content in the filtrate was measured using the iFAMs system.

Time Dependency of Gliadin Solubility in Tris Buffer with and without IL. We investigated the effect of extraction time on gliadin solubility in 1% $[C5DMIM][OMs]_{aq}$ and Tris buffer. For each buffer, we added 3 g of gliadin to separate sample vials and homogenized the mixtures by shaking. The mixtures were then allowed to rest for various time intervals (0.5, 1, 3, 5, 7, 10, 20, and 40 min). Precipitates were removed using a 0.22 μm filter, and gliadin solubility was determined by using a lateral flow assay. Results were quantified using an image analysis software tool (color intensity assay on Web site).

As a control, we repeated the experiment using PBS buffer in place of $[C5DMIM][OMs]_{aq}$, following the same extraction procedure and analysis methods.

Recovery Test of the iFAMs. Rice noodles are gluten-free, and they were thus selected as a substrate to evaluate the gliadin recovery efficiency of the iFAMs system.

Hydrophobic proteins are traditionally extracted using alcohol solutions. For this experiment, we prepared a 75 wt % ethanol solution. Subsequently, 3 g of bread flour (Blue Jacket Strong Flour, Lien Hwa Milling) was mixed with 10 mL of this solution, followed by extraction at room temperature for 5 min. The mixture was centrifuged (8500 rpm, 3 min) and filtered (0.22 μm pore size) to obtain a clear gliadin extract. The gliadin concentration was determined using a wheat/gluten (gliadin) ELISA kit (Crystal Chem, AOAC no. 011804). Samples were diluted by at least 50-fold to ensure accurate quantification. The gliadin concentrations in both 75

https://doi.org/10.1021/acsomega.4c08411
ACS Omega 2024, 9, 49767−49777

wt % ethanol extraction groups exceeded 1700 ppm. In addition, 40 g of dried gluten-free rice noodles (Organic Rice Noodles, Yuan Shun Food) was rehydrated in water. After draining, the noodles were soaked in 10 mL of a 10 ppm gliadin solution (prepared in 100% ethanol) at room temperature. Owing to their high specific surface area, the rice noodles effectively adsorbed the gliadin. After the ethanol solvent was evaporated, the gliadin-spiked rice noodles were lyophilized. The lyophilized gliadin-spiked rice noodles were analyzed by using the iFAMs at room temperature to assess gliadin recovery.

■ ASSOCIATED CONTENT

Supporting Information

The Supporting Information is available free of charge at https://pubs.acs.org/doi/10.1021/acsomega.4c08411.

Figure S1: smartphone image assay; Figure S2: cost of gluten test by Tris and new extraction buffer systems; Figure S3: competitive assay of iFAMs, rapid test, and ELISA (DOCX)

■ AUTHOR INFORMATION

Corresponding Author

Yu-Cheng Hsiao − *Graduate Institute of Biomedical Optomechatronics and Cell Physiology and Molecular Image Research Center, Taipei Medical University, Taipei 110, Taiwan; School of Biological Sciences, Nanyang Technological University, 639798, Singapore;* orcid.org/0000-0003-3312-7318; Email: ychsiao@tmu.edu.tw

Authors

Wen-Hao Chen − *Research and Development Group, Leo Verification Systems Inc., Powell, Wyoming 82435, United States; School of Biological Sciences, Nanyang Technological University, 639798, Singapore*

Chuan-Chih Hsu − *Department of Surgery, College of Medicine, Taipei Medical University, Taipei 110, Taiwan; Department of Surgery, Taipei Medical University Hospital, Taipei 110, Taiwan*

Hsin-Jung Ho − *Technology Commercialization Center, Taipei Medical University, Taipei 110, Taiwan*

Jill Smith − *Research and Development Group, Leo Verification Systems Inc., Powell, Wyoming 82435, United States*

Seaton Smith − *Research and Development Group, Leo Verification Systems Inc., Powell, Wyoming 82435, United States*

Hui-Yin Huang − *Research and Development Group, Leo Verification Systems Inc., Powell, Wyoming 82435, United States*

Huan-Chi Chang − *uMeal Co., Ltd., Taipei 110, Taiwan*

Complete contact information is available at: https://pubs.acs.org/10.1021/acsomega.4c08411

Author Contributions

[+]W.-H.C., C.-C.H., and H.-J.H. contributed equally to this work.

Notes

The authors declare no competing financial interest.

■ ACKNOWLEDGMENTS

We thank Chester Y. C. Chu (Director of the State of Wyoming—Asia Pacific Trade Office) for helping us contact the following founders: Sam Clickman (founder of Big Lost Meadery & Brewery), Chas Marsh (founder of Jackson Hole Still Works), and Eli Dicklich (founder of Pine Ridge Barbecue & Dipping Sauces). We thank the founders as well for providing the required samples. Furthermore, we thank Jill Smith and Seaton Smith for their assistance with sample testing in the United States. We acknowledge the Laboratory Animal Center at TMU for technical support in antibody development.

■ REFERENCES

(1) Krogulska, A.; Wood, R. A.; Sampson, H. Peanut allergy diagnosis: Moving from basic to more elegant testing. *Pediatr. Allergy Immunol.* **2020**, *31* (4), 346−357.

(2) Midun, E.; et al. Recent advances in the management of nut allergy. *World Allergy Organ. J.* **2021**, *14* (1), No. 100491.

(3) Zhang, Z.; et al. Seafood allergy: Allergen, epitope mapping and immunotherapy strategy. *Crit. Rev. Food Sci. Nutr.* **2023**, *63* (10), 1314−1338.

(4) Cárdenas-Torres, F. I.; et al. Non-celiac gluten sensitivity: An update. *Medicina* **2021**, *57* (6), 526.

(5) Cabanillas, B. Gluten-related disorders: Celiac disease, wheat allergy, and nonceliac gluten sensitivity. *Crit. Rev. Food Sci. Nutr.* **2020**, *60* (15), 2606−2621.

(6) Amundarain, M. J.; et al. IDP Force Fields Applied to Model PPII-Rich 33-mer Gliadin Peptides. *J. Phys. Chem. B* **2023**, *127* (11), 2407−2417.

(7) Besser, H. A.; Khosla, C. Celiac disease: Mechanisms and emerging therapeutics. *Trends Pharmacol. Sci.* **2023**, *44*, 949.

(8) Tamai, T.; Ihara, K. Celiac Disease Genetics, Pathogenesis, and Standard Therapy for Japanese Patients. *Int. J. Mol. Sci.* **2023**, *24* (3), 2075.

(9) Wieser, H.; Koehler, P.; Scherf, K. A. Chemistry of wheat gluten proteins: Quantitative composition. *Cereal Chem.* **2023**, *100* (1), 36−55.

(10) Kłosok, K.; et al. Effects of physical and chemical factors on the structure of gluten, gliadins and glutenins as studied with spectroscopic methods. *Molecules* **2021**, *26* (2), 508.

(11) Wouters, A. G. B.; Joye, I. J.; Delcour, J. A. Understanding the air-water interfacial behavior of suspensions of wheat gliadin nanoparticles. *Food Hydrocolloids* **2020**, *102*, No. 105638.

(12) Výrostková, J.; et al. Detection of Gluten in Gluten-Free Foods of Plant Origin. *Foods* **2022**, *11* (14), 2011.

(13) Gabler, A.; Scherf, K. Comparative characterization of gluten and hydrolyzed wheat proteins. *Biomolecules* **2020**, *10* (9), 1227.

(14) Bariani, G. C.; et al. Patterning large-scale nanostructured microarrays on coverslip for sensitive plasmonic detection of aqueous gliadin traces. *Chemosensors* **2022**, *10* (2), 38.

(15) Hong, S. P.; Keasberry, N. A.; Ahmed, M. U. Development of a gliadin immunosensor incorporating gold nanourchin, molybdenum disulfide, titanium dioxide, and Nafion for enhanced electrochemiluminescence. *Microchem. J.* **2023**, *193*, No. 109059.

(16) Svigelj, R.; et al. An effective label-free electrochemical aptasensor based on gold nanoparticles for gluten detection. *Nanomaterials* **2022**, *12* (6), 987.

(17) Jang, Y.-R.; et al. High-throughput analysis of high-molecular weight glutenin subunits in 665 wheat genotypes using an optimized MALDI-TOF−MS method. *3 Biotech* **2021**, *11*, 1−8.

(18) Wu, Q.; et al. Reagent-free detection of multiple allergens in gluten-free flour using NIR spectroscopy and multivariate analysis. *J. Food Compos. Anal.* **2023**, *120*, No. 105324.

(19) Lin, H.-Y.; et al. Integrated magneto-chemical sensor for on-site food allergen detection. *ACS Nano* **2017**, *11* (10), 10062−10069.

(20) Tertis, M.; et al. Innovative nanostructured aptasensor for the electrochemical detection of gluten in food samples. *Microchem. J.* **2023**, *193*, No. 109069.
(21) Amnuaycheewa, P.; et al. Challenges in Gluten Analysis: A Comparison of Four Commercial Sandwich ELISA Kits. *Foods* **2022**, *11* (5), 706.
(22) Huang, X.; et al. Quantification of barley contaminants in gluten-free oats by four gluten ELISA kits. *J. Agric. Food Chem.* **2022**, *70* (7), 2366−2373.
(23) Momeni, A.; et al. Gold-based nanoplatform for a rapid lateral flow immunochromatographic test assay for gluten detection. *BMC Biomed. Eng.* **2022**, *4* (1), 5.
(24) Hu, J.; et al. Gold nanoparticle-based lateral flow immunoassay for the rapid and on-site detection of wheat allergen in milk. *Food Biosci.* **2023**, *51*, No. 102353.
(25) YOCKELL-LELIÈVRE, H.; LUSSIER, F.; MASSON, J.-F. Influence of the particle shape and density of self-assembled gold nanoparticle sensors on LSPR and SERS. *J. Phys. Chem. C* **2015**, *119* (51), 28577−28585.
(26) Koushki, E.; Koushki, A. Simple method for optical detection and characterization of surface agents on conjugated gold nanoparticles. *Plasmonics* **2023**, 1151−1157.
(27) Chutimasakul, T.; et al. Size-controlled preparation of gold nanoparticles deposited on surface-fibrillated cellulose obtained by citric acid modification. *ACS Omega* **2020**, *5* (51), 33206−33213.
(28) Okyem, S.; et al. High-affinity points of interaction on antibody allow synthesis of stable and highly functional antibody−gold nanoparticle conjugates. *Bioconjugate Chem.* **2021**, *32* (8), 1753−1762.
(29) Nurrohman, D. T.; Chiu, N. F. Interaction Studies of Localized Surface Plasmon Resonance Immunosensor Based on Gold Nanoparticles. *IEEE Sens. J.* **2023**, *23*, 19262.
(30) Wieser, H.; et al. Food safety and cross-contamination of gluten-free products: A narrative review. *Nutrients* **2021**, *13* (7), 2244.
(31) Fritz, R. D.; Chen, Y. Commentary: to be oats or not to be? An update on the ongoing debate on oats for patients with celiac disease. *Front. Pediatr.* **2020**, *8*, No. 573151.
(32) Raju, N.; et al. Gluten contamination in labelled and naturally gluten-free grain products in southern India. *Food Addit. Contam.: Part A* **2020**, *37* (4), 531−538.
(33) Yu, J.-T.; et al. Molecular dynamics simulation of α-gliadin in ethanol/aqueous organic solvents. *Int. J Food Sci. Technol.* **2023**, *58* (2), e1−e9.
(34) Einali, A. R.; Sadeghipour, H. R. Alleviation of dormancy in walnut kernels by moist chilling is independent from storage protein mobilization. *Tree Physiol.* **2007**, *27*, 519−525.
(35) FU, B. X.; SAPIRSTEIN, H. D.; BUSHUK, W. Salt-induced disaggregation solubilization of gliadin and glutenin proteins in water. *Journal of Cereal Science* **1996**, *24* (3), 241−246.
(36) Majzoobi, M.; et al. Functional properties of acetylated glutenin and gliadin at varying pH values. *Food Chem.* **2012**, *133* (4), 1402−1407.
(37) Sahin, E.; et al. Comparative effects of pH and ionic strength on protein−protein interactions, unfolding, and aggregation for IgG1 antibodies. *J. Pharm. Sci.* **2010**, *99* (12), 4830−4848.
(38) Wang, T.; et al. Effect of ionic strength and pH on the physical and chemical stability of a monoclonal antibody antigen-binding fragment. *J. Pharm. Sci.* **2013**, *102* (8), 2520−2537.
(39) LAUBE, T.; et al. Magneto immunosensor for gliadin detection in gluten-free foodstuff: Towards food safety for celiac patients. *Biosens. Bioelectron.* **2011**, *27* (1), 46−52.
(40) de Lourdes Moreno, M.; et al. Detection of gluten immunogenic peptides in the urine of patients with coeliac disease reveals transgressions in the gluten-free diet and incomplete mucosal healing. *Gut* **2015**, *66*, 250.
(41) Scherf, K. A.; Poms, R. E. Recent developments in analytical methods for tracing gluten. *J. Cereal Sci.* **2016**, *67*, 112−122.
(42) Tirkey, A.; Babu, P. J. Synthesis and characterization of citrate-capped gold nanoparticles and their application in selective detection of creatinine (A kidney biomarker). *Sens. Int.* **2024**, *5*, No. 100252.
(43) Chen, W.-H.; et al. Optimizing Gluten Extraction Using Eco-friendly Imidazolium-Based Ionic Liquids: Exploring the Impact of Cation Side Chains and Anions. *ACS Omega* **2024**, 17028.

https://doi.org/10.1021/acsomega.4c08411
ACS Omega 2024, 9, 49767−49777